INTERNATIONAL JOURNAL FOR NUMERICAL METHODS IN FLUIDS
Int. J. Numer. Meth. Fluids 2003; **43**:1081–1098 (DOI: 10.1002/fld.547)

Implicit kinetic schemes for the Euler equations

H. S. R. Reksoprodjo[1] and R. K. Agarwal[2,*,†]

[1]*Graduate Research Assistant, National Institute for Aviation Research, Wichita State University, Wichita, KS 67260-0093, U.S.A.*
[2]*Department of Mechanical Engineering, Washington University, St. Louis, MO 63130, U.S.A.*

SUMMARY

Recently, the kinetic schemes, namely the kinetic flux-vector split (KFVS) scheme and kinetic wave/particle split (KWPS) scheme, for Euler flows have gained wide recognition for their efficiency and robustness. However, to date, all computations performed with these schemes have employed a time-explicit formulation. The explicit kinetic schemes severely restrict the time-step allowed for stability. In this paper, an implicit formulation is derived for both the KFVS and KWPS schemes, and is applied to compute the shock tube and shock structure problems in one-dimension, and oblique shock reflection from a flat plate and supersonic flow past a blunt-body in two dimensions. Results are compared with analytical results where available and solutions from explicit formulations. It is shown that implicit formulations retain the efficiency and robustness of their explicit counterparts without the restrictive time step constraints. This results in an increase in computational speed for steady state computations. To the authors' knowledge, this is the first time that the implicit kinetic schemes have been formulated.

KEY WORDS: implicit schemes; kinetic schemes; Euler equations; Boltzmann equation

1. INTRODUCTION

In recent years, there has been considerable interest in the kinetic schemes for solving the Euler and Navier–Stokes equations. However, to date, all the papers on kinetic schemes reported in the literature employ an explicit formulation due to its simplicity. The major drawback of the explicit formulation is the restriction placed on the time-step allowed for the stability of the scheme.

Kinetic schemes are based on the fact that the set of equations governing the motion of fluid flows at the continuum level, i.e. Euler, Navier–Stokes, and Burnett equations, can be obtained by taking the moments of the Boltzmann equation at the molecular level with respect to the collision invariants. This is often referred to as the '*moment method strategy*'. For gas in the state of collisional equilibrium, the collision integral vanishes, and the Boltzmann

* Correspondence to: R. K. Agarwal, Department of Mechanical Engineering, Washington University, Campus Box 1185, 1 Brookings Drive, St. Louis, MO 63130, U.S.A.
† E-mail: rka@me.wustl.edu

Received 3 March 2002
Revised 17 February 2003

equation adopts a form similar to that of the linear wave equation. Its solution is simply the Maxwellian probability density distribution function. When moments of this equation are taken with the collision invariants, the Euler equations are obtained.

One of the well-known and extensively used kinetic schemes, the kinetic flux-vector splitting (KFVS) scheme proposed by Deshpande [1], splits the flux term in the Boltzmann equation into positive and negative parts based on the sign of the molecular velocity. Taking the moments of this split flux with respect to the collision invariant vector results in the KFVS algorithm. This scheme, however, requires the evaluation of the computationally expensive error functions.

Recently, Agarwal and Acheson [2] have proposed a new flux splitting at Boltzmann level, which they call kinetic wave/particle splitting (KWPS). They have shown that this new splitting does not lead to the evaluation of error functions, which results in increased computational speed and also simplifies the algebra considerably. By recognizing that the molecular velocity of an individual gas particle can be expressed as the sum of the average fluid velocity of the gas and each particle's thermal (peculiar) velocity, the Boltzmann flux can be split into two components: the convective part and the acoustic part. These two parts of the Boltzmann flux are then upwind discretized and the moments of this discretized equation with the collision invariants then result in the KWPS scheme for the Euler equations.

The schemes mentioned above have been investigated using explicit formulations. This necessitates limiting the time step for the sake of stability. Implicit flow solvers do not suffer from this drawback, allowing larger time-step, and thereby significantly reducing the computation time for a wide range of flow problems. Therefore, it is desirable to derive implicit formulations for the kinetic schemes, for both the KFVS and the KWPS schemes.

In this paper, for the first time, implicit formulations of two kinetic schemes, namely the KFVS scheme and the KWPS scheme, are systematically derived. For simplicity, in this paper the derivations are presented in one-dimension only. Extensions of the algorithms to 2-D and 3-D Euler equations are straightforward. The implicit KFVS and KWPS algorithms are then numerically tested for accuracy and robustness. The test cases include the 1-D shock tube, 1-D shock structure, the 2-D oblique shock reflection from a flat plate, and 2-D supersonic flow past a blunt-body.

2. DERIVATIONS OF THE SCHEMES

This section describes the systematic derivation of implicit formulations of two kinetic schemes, i.e. KFVS scheme and the KWPS scheme, for the Euler equations. For simplicity, the derivation is given in one-dimension only. Extensions to 2-D and 3-D are straightforward. The implicit KFVS and KWPS algorithms are then numerically tested for accuracy. Two different approaches are employed in the derivations.

In the macroscopic approach, the Jacobian matrices are simply obtained from the split flux-vectors at the continuum level. In the microscopic approach, an implicit algorithm is first devised for solving the Boltzmann equation. The moment method strategy is then employed to obtain the Jacobian matrices. It will be shown that in the case of KFVS scheme, either approach gives identical results. However, this is not the case for the KWPS scheme. This arises from the fact that the split-flux vectors are not continuously differentiable with respect to the state variables.

2.1. Kinetic schemes

The Boltzmann equation, which governs the molecular motion, can be written as follows:

$$\frac{\partial f}{\partial t} + v_i \frac{\partial f}{\partial x_i} = J(f, f) \tag{1}$$

For gas in collisional equilibrium, the right hand side vanishes, and the solution is simply a Maxwellian distribution function:

$$f^{(0)} = \rho \frac{1}{\varepsilon_o} \exp\left(-\frac{\varepsilon}{\varepsilon_o}\right) \left(\frac{\beta}{\pi}\right)^{3/2} \exp(-\beta(v_k - u_k)(v_k - u_k)) \tag{2}$$

where the average internal energy is expressed as $\varepsilon_o = (1/(\gamma - 1) - \frac{3}{2})\frac{1}{2\beta}$.

Define the moment method strategy as the following operation:

$$\langle \boldsymbol{\Psi}, f \rangle \equiv \int_{\Re^+} \mathrm{d}\varepsilon \int_{\Re^3} \mathrm{d}^3 v_i (\boldsymbol{\Psi} f) \tag{3}$$

When this operation is applied to Equation (1) with the Maxwellian distribution function (2), the Euler equations are obtained.

For simplicity, the following derivation is given in one dimension only, which implies that 2 of the velocity components, namely u_y and u_z vanish. In this situation, the Maxwellian distribution function simplifies to

$$f^{(0)} = \rho \frac{1}{\varepsilon_o} \exp\left(-\frac{\varepsilon}{\varepsilon_o}\right) \left(\frac{\beta}{\pi}\right)^{1/2} \exp(-\beta(v_x - u_x)^2) \tag{4}$$

where the average internal energy is expressed as $\varepsilon_o = (1/(\gamma - 1) - \frac{1}{2})\frac{1}{2\beta}$. Furthermore, the moment method strategy operation (3) is simplified to

$$\langle \boldsymbol{\Psi}, f \rangle \equiv \int_{\Re^+} \mathrm{d}\varepsilon \int_{\Re} \mathrm{d}v_x (\boldsymbol{\Psi} f) \tag{5}$$

where the collision invariant vector now becomes $\boldsymbol{\Psi} = [1 \;\; v_x \;\; \varepsilon + \frac{1}{2}v_x^2]^{\mathrm{T}}$.

Operation (5) results in 1-D Euler equations which can be expressed as

$$\frac{\partial \mathbf{Q}}{\partial t} + \frac{\partial \mathbf{F}}{\partial x} = \mathbf{0} \tag{6}$$

where

$$\mathbf{Q} = \begin{bmatrix} \rho \\ \rho u_x \\ \rho e_t \end{bmatrix} \quad \text{and} \quad \mathbf{F} = \begin{bmatrix} \rho u_x \\ \rho u_x^2 + p \\ \rho u_x e_t + p u_x \end{bmatrix}$$

Note that in all derivations the equation of state for ideal gas ($p = \rho RT$) is assumed to hold.

The KFVS scheme is derived by first splitting the flux vector in the Boltzmann equation (1) into positive and negative molecular velocity spaces and then taking the

moments. The resulting flux vector in the Euler equations is now split into two parts, one corresponding to the positive space, and the other corresponding to the negative space:

$$\frac{\partial \mathbf{Q}}{\partial t} + \frac{\partial \mathbf{F}^+}{\partial x} + \frac{\partial \mathbf{F}^-}{\partial x} = \mathbf{0} \tag{7}$$

The resulting split flux-vectors for the KFVS scheme can be expressed as

$$\mathbf{F}^{\pm} = \frac{1 \pm \mathrm{erf}(S_x)}{2} \begin{bmatrix} \rho u_x \\ \rho u_x^2 + p \\ \rho u_x e_t + p u_x \end{bmatrix} \pm \frac{\exp(-S_x^2)}{2\sqrt{\pi\beta}} \begin{bmatrix} \rho \\ \rho u_x \\ \rho e_t + \frac{1}{2} p \end{bmatrix} \tag{8}$$

where $S_x = u_x \sqrt{\beta}$ and $\mathrm{erf}(s) = \frac{2}{\sqrt{\pi}} \int_0^s \mathrm{d}t \exp(-t^2)$.

On the other hand, in deriving the KWPS scheme, the molecular velocity (v_i) is first decomposed into fluid velocity (u_i) and thermal velocity (c_i) as $v_i = u_i + c_i$ [3]. Both the fluid and thermal velocity are split into positive and negative spaces, and then the moments are taken. Then, the resulting flux-vectors in the Euler equations can be expressed as

$$\mathbf{F}^{\pm} = \frac{u_x \pm |u_x|}{2} \begin{bmatrix} \rho \\ \rho u_x \\ \rho e_t \end{bmatrix} + \frac{1}{2} \begin{bmatrix} 0 \\ p \\ p u_x \end{bmatrix} \pm \frac{1}{2\sqrt{\pi\beta}} \begin{bmatrix} \rho \\ \rho u_x \\ \rho e_t + \frac{1}{2} p \end{bmatrix} \tag{9}$$

2.2. Explicit formulation

The Equation (7) is generally solved using a time marching scheme, in which the solution is updated at each time level using the flux terms. In the explicit formulation, these flux terms are evaluated at current time level as follows:

$$\Delta \mathbf{Q}_j = \mathbf{Q}_j^{n+1} - \mathbf{Q}_j^n = -\frac{\Delta t}{\Delta x} (\mathbf{F}_j^+ - \mathbf{F}_{j-1}^+ + \mathbf{F}_{j+1}^- - \mathbf{F}_j^-)^n \tag{10}$$

This explicit formulation for the kinetic schemes has been successfully applied to compute the Euler flows for over a decade by many researchers.

2.3. Implicit formulation

In the implicit formulation, the flux terms at the next time level are employed in the updating process. Thus:

$$\Delta \mathbf{Q}_j = -\frac{\Delta t}{\Delta x} (\mathbf{F}_j^+ - \mathbf{F}_{j-1}^+ + \mathbf{F}_{j+1}^- - \mathbf{F}_j^-)^{n+1} \tag{11}$$

To evaluate expression (11), a linearization of the flux vectors with respect to the state variable vector is employed, which requires the computation of the Jacobian matrices.

There are two approaches to derive the implicit kinetic schemes: first is based on obtaining the Jacobian matrices from the split flux-vectors at the continuum ($\mathscr{C}$) level; and the second approach first derives the implicit scheme for the Boltzmann equation at the molecular ($\mathscr{M}$) level and then takes the moments with respect to the collision invariants ($\boldsymbol{\Psi}$).

First, the implicit scheme using the macroscopic approach is derived. The split Jacobians are obtained by linearization of the split flux vectors at the continuum level. The procedure here follows the one given in Hoffman and Chiang [4]. The results are as follows:

$$(\mathbf{F}^{\pm})^{n+1} \approx (\mathbf{F}^{\pm})^{n} + \Delta t \frac{\partial \mathbf{F}^{\pm}}{\partial t} \approx (\mathbf{F}^{\pm})^{n} + \Delta t \frac{\partial \mathbf{F}^{\pm}}{\partial \mathbf{Q}} \frac{\partial \mathbf{Q}}{\partial t} \approx (\mathbf{F}^{\pm})^{n} + \mathbf{A}^{\pm} \Delta \mathbf{Q} \tag{12}$$

This approach is very straightforward; the resulting 1-D Jacobian matrices are given below. For brevity, the Jacobian matrix $\mathbf{A}$ is given as the following matrix product:

$$\mathbf{A} = \mathbf{B}\mathbf{C}^{-1} \tag{13}$$

where

$$\mathbf{C} = \begin{bmatrix} 1 & 0 & 0 \\ u_x & 1 & 0 \\ q & u_x & \frac{1}{\gamma - 1} \end{bmatrix}$$

For KFVS scheme:

$$\mathbf{A}^{\pm} = \frac{1 \pm \operatorname{erf}(S_x)}{2} \mathbf{A}_1 \pm \frac{\exp(-S_x^2)}{2\sqrt{\pi\beta}} \mathbf{A}_2 = \left[\frac{1 \pm \operatorname{erf}(S_x)}{2} \mathbf{B}_1 \pm \frac{\exp(-S_x^2)}{2\sqrt{\pi\beta}} \mathbf{B}_2 \right] \mathbf{C}^{-1} \tag{14}$$

where

$$\mathbf{B}_1 = \begin{bmatrix} u_x & 1 & 0 \\ u_x^2 & 2u_x & 1 \\ u_x q & u_x^2 + e_t + \frac{1}{2\beta} & \frac{1}{\gamma - 1} u_x + u_x \end{bmatrix}$$

$$\mathbf{B}_2 = \begin{bmatrix} \frac{1}{2} & 0 & \beta \\ u_x & 2 & 0 \\ q + \frac{1}{4}u_x^2 - \frac{1}{2}e_t - \frac{1}{8\beta} & \frac{3}{2}u_x & \frac{1}{\gamma - 1} - \frac{1}{2}u_x^2\beta + e_t\beta + \frac{3}{4} \end{bmatrix}$$

For KWPS scheme:

$$\mathbf{A}^{\pm} = \frac{1 \pm \operatorname{sgn}(u_x)}{2} \mathbf{A}_0 + \frac{1}{2}\mathbf{A}_1 \pm \frac{1}{2\sqrt{\pi\beta}} \mathbf{A}_2 = \left[\frac{1 \pm \operatorname{sgn}(u_x)}{2} \mathbf{B}_0 + \frac{1}{2}\mathbf{B}_1 \pm \frac{1}{2\sqrt{\pi\beta}} \mathbf{B}_2 \right] \mathbf{C}^{-1} \tag{15}$$

where

$$\mathbf{B}_0 = \begin{bmatrix} u_x & 1 & 0 \\ u_x^2 & 2u_x & 0 \\ u_x q & u_x^2 + e_t & \frac{1}{\gamma - 1} u_x \end{bmatrix}$$

$$\mathbf{B}_1 = \begin{bmatrix} 0 & 0 & 0 \\ 0 & 0 & 1 \\ 0 & \frac{1}{2\beta} & u_x \end{bmatrix}$$

$$\mathbf{B}_2 = \begin{bmatrix} \frac{1}{2} & 0 & \beta \\ \frac{1}{2}u_x & 1 & u_x\beta \\ q - \frac{1}{2}e_t - \frac{1}{8\beta} & u_x & \frac{1}{\gamma-1} + e_t\beta + \frac{3}{4} \end{bmatrix}$$

Note that when $u_x = 0$, $\mathbf{A}_0 \equiv [\mathbf{0}]$.

Using Equation (12), Equation (11) can now be written as the following block tri-diagonal system of equations:

$$\mathrm{X}\Delta\mathbf{Q}_{j-1} + \mathrm{Y}\Delta\mathbf{Q}_j + \mathrm{Z}\Delta\mathbf{Q}_{j+1} = \mathrm{RHS} \tag{16}$$

where

$$\mathrm{X} = -\frac{\Delta t}{\Delta x}\mathbf{A}^+_{j-1}$$

$$\mathrm{Y} = [\mathbf{I}] + \frac{\Delta t}{\Delta x}(\mathbf{A}^+_j - \mathbf{A}^-_j)$$

$$\mathrm{Z} = +\frac{\Delta t}{\Delta x}\mathbf{A}^-_{j+1}$$

$$\mathrm{RHS} = -\frac{\Delta t}{\Delta x}(\mathbf{F}^+_j - \mathbf{F}^+_{j-1} + \mathbf{F}^-_{j+1} - \mathbf{F}^-_j)^n$$

The alternate approach to deriving the implicit kinetic scheme for the Euler equations is to first construct the implicit scheme for the Boltzmann equation (1), and then take the moments. In this case, one needs to express the change in the Maxwellian distribution ($\mathrm{d}f^{(0)}$) in terms of the change in the state variable ($\mathrm{d}\mathbf{Q}$), expressed as

$$\mathrm{d}f^{(0)} = a_m\mathrm{d}(\rho) + a_x\mathrm{d}(\rho u_x) + a_E\mathrm{d}(\rho e_t) \tag{17}$$

where

$$a_m = f^{(0)}\left(\frac{1+\Phi}{\rho} - \frac{2\beta}{\rho}c_x u_x - \frac{\gamma-1}{\rho}2\beta\Phi q\right)$$

$$a_x = f^{(0)}\left(\frac{2\beta}{\rho}c_x + \frac{\gamma-1}{\rho}2\beta\Phi u_x\right)$$

$$a_E = f^{(0)}\left(-\frac{\gamma-1}{\rho}\,2\beta\Phi\right)$$

$$\Phi = \frac{3}{2} - \frac{\varepsilon}{\varepsilon_o} - \beta c_x^2$$

Note that the resulting system after taking the moments again has the same form as equation (16).

In the case of KFVS scheme, this results in an identical expression for the Jacobian matrices. On the other hand, for the KWPS scheme, the following expressions are obtained:

$$\mathbf{A}^{\pm} = \frac{u_x \pm |u_x|}{2}[\mathbf{I}] + \frac{1}{2}\mathbf{A}_1 \pm \frac{1}{2\sqrt{\pi\beta}}\,\mathbf{A}_2 = \frac{u_x \pm |u_x|}{2}[\mathbf{I}] + \left[\frac{1}{2}\,\mathbf{B}_1 \pm \frac{1}{2\sqrt{\pi\beta}}\,\mathbf{B}_2\right]\mathbf{C}^{-1} \tag{18}$$

where

$$\mathbf{B}_1 = \begin{bmatrix} 0 & 1 & 0 \\ 0 & u_x & 1 \\ 0 & e_t + \frac{1}{2\beta} & u_x \end{bmatrix}$$

$$\mathbf{B}_2 = \begin{bmatrix} \frac{1}{2} & 0 & \beta \\ \frac{1}{2}u_x & 2 & u_x\beta \\ q - \frac{1}{2}e_t - \frac{1}{8\beta} & 2u_x & \frac{1}{\gamma-1} + e_t\beta + \frac{3}{4} \end{bmatrix}$$

To the best of the authors' knowledge, the implicit kinetic schemes as expressed above have never been formulated in the literature before.

3. NUMERICAL VALIDATION OF THE SCHEMES: 1- AND 2-D TEST CASES

To investigate the new implicit algorithms, a series of numerical tests is conducted. The first test is to compare the accuracy of the implicit schemes in a time accurate fashion with the explicit schemes. For this purpose, the 1-D shock tube test case is employed, with density and pressure ratios of $\rho_L/\rho_R = 8$ and $p_L/p_R = 10$, respectively. A grid with $L = 2000$ points is employed. This high level of resolution is chosen to allow the implicit schemes enough time to evolve. The time step is $\Delta t = 0.4$ for the explicit schemes, which roughly corresponds to CFL ≈ 0.877, and $\Delta t = 8.0$ for the implicit schemes. Final solution is obtained at $t = 400$.

Since the main advantage of implicit schemes over explicit schemes is in the computation of steady state solutions, another test case with a steady state solution is computed. For this purpose, a Mach 1.5 steady shock within a channel is computed. The domain consists of $L = 100$ grid points. For Euler flows, an analytical solution exists, and can be found in standard textbooks on compressible fluid flow, e.g. the book by Anderson [5]. To start the flow at $t = 0$, linear variations in density, velocity, and pressure spanning the domain are created, and the boundary conditions are then set to the analytical values. For the purpose

of comparison, the L_2-*norm* of density change is computed at every time step. For explicit schemes, a time step of $\Delta t = 0.3$, which roughly corresponds to CFL ≈ 0.89 is employed. A time step of $\Delta t = 3.0$ is used for the implicit schemes. The solution is assumed to converge when L_2-norm $< 10^{-5}$.

In 2-D, first a simple test case of an oblique shock reflecting from a flat plate is considered. The computational domain is of 4×1 units, which is discretized into 321×101 points. An oblique shock wave enters from the top left corner at an angle of 29° and is reflected by the flat plate. The farfield flow is a steady Mach 2.9 flow from left to right. For the explicit schemes, CFL $= 0.4$ is employed, while CFL $= 40.0$ is used for the implicit schemes. The solution is assumed to converge when the L_2-norm of changes in density is less than 10^{-7}.

Finally, the supersonic flow past a 2-D blunt-body is computed. The leading edge is semi-circular with a radius $R = 0.1$ m, and the afterbody extends to $2R$ behind the leading edge. The grid consists of 78×51 points. The inflow conditions are set to that of a uniform flow of Mach 5.85 with farfield density and pressure values of $T_\infty = 55$ K and $p_\infty = 510$ Pa. The CFL values used are 0.4 for the explicit schemes and 2.0 for the implicit schemes. The solution is assumed to converge when the L_2-norm of changes in density is less than 10^{-7}. Only the KWPS schemes are used to compute this test case.

In computations using the implicit schemes, the block tridiagonal system is solved using the routines provided in Tannehill *et al.* [6]. Also, the routine for the error functions calculations needed in KFVS formulations is taken from Press *et al.* [7], which is based on Chebyshev fitting.

4. NUMERICAL RESULTS AND DISCUSSION

For the shock tube test case, analytical solutions are employed for comparison with the numerical results. From the solutions obtained with the implicit schemes, shown in Figures 1 and 2, and those obtained with the explicit schemes, shown in Figures 3 and 4, it is clear that the implicit schemes are able to produce very accurate results at a significantly larger time step compared to the explicit schemes, despite not being able to capture some of the transient details at the initial time steps as expected.

To better demonstrate the advantage of the implicit schemes, results from the steady state shock structure computations are presented. The results from the implicit schemes, Figures 5 and 6, show no noticable difference with their explicit counterparts, Figures 7 and 8. However, the implicit schemes show significantly more rapid convergence rates compared to explicit schemes, as shown in Figure 9 and Table I.

Density contours for the 2-D oblique shock reflection from a flat plate obtained using the implicit schemes are presented in Figures 10 and 11. These results are essentially identical to those obtained using the explicit schemes. However, the convergence history data, shown in Figures 12–14 and Table II, show faster convergence rates for the implicit schemes.

For supersonic flow past a 2-D blunt-body, the density contour plots are presented in Figure 15 for the explicit and the implicit KWPS scheme. The stagnation line profiles for the density, thermal pressure, and temperature are given in Figures 16 and 17 for the explicit and implicit KWPS scheme respectively. It is clear that both the implicit and explicit scheme produce indistinguishable results. The convergence histories for the explicit and implicit KWPS schemes are given in Figure 18. The computation time is presented in Table III. It is clear

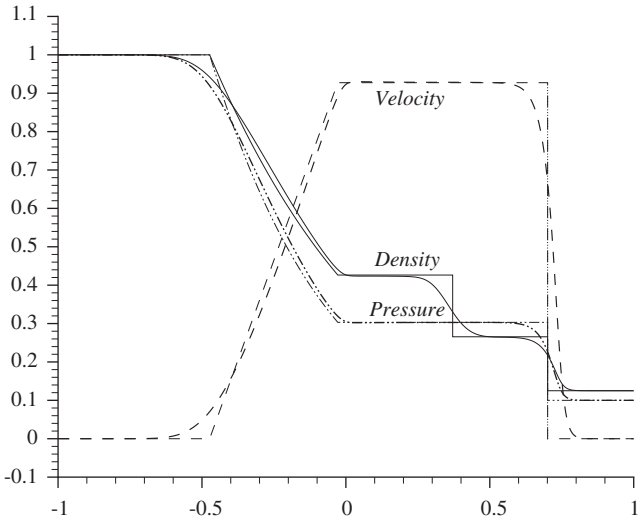

Figure 1. Implicit KFVS calculations for the 1-D shock tube test case: comparison of analytical solutions and computational results.

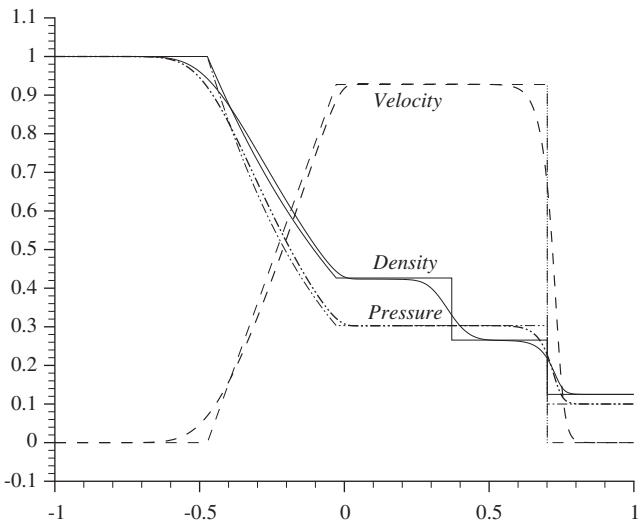

Figure 2. Implicit KWPS calculations for the 1-D shock tube test case: comparison of analytical solutions and computational results.

that although the implicit scheme requires less number of time steps to achieve the steady-state solution, it still takes more CPU time to converge to the final solution. However, with increasing number of grid points, it is expected that the implicit scheme will become a more attractive alternative.

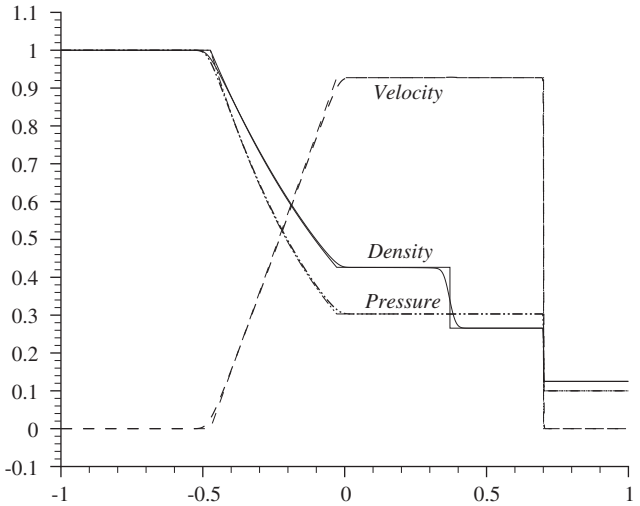

Figure 3. Explicit KFVS calculations for the 1-D shock tube test case: comparison of analytical solutions and computational results.

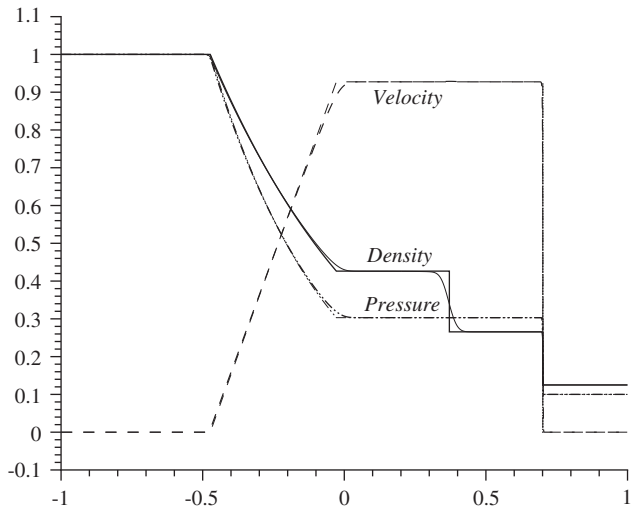

Figure 4. Explicit KWPS calculations for the 1-D shock tube test case: comparison of analytical solutions and computational results.

Comparing the two kinetic schemes, kinetic flux-vector split and kinetic wave/particle split, it is clear that KFVS tends to be more accurate than the more diffusive KWPS on the same grid. This, however, comes at a price of calculating the numerically expensive error functions in the KFVS scheme.

From comparison of results from the two variants of implicit KWPS scheme, ($\mathscr{C}$) and ($\mathscr{M}$), it is found that the molecular ($\mathscr{M}$) approach is preferable to the continuum ($\mathscr{C}$) approach.

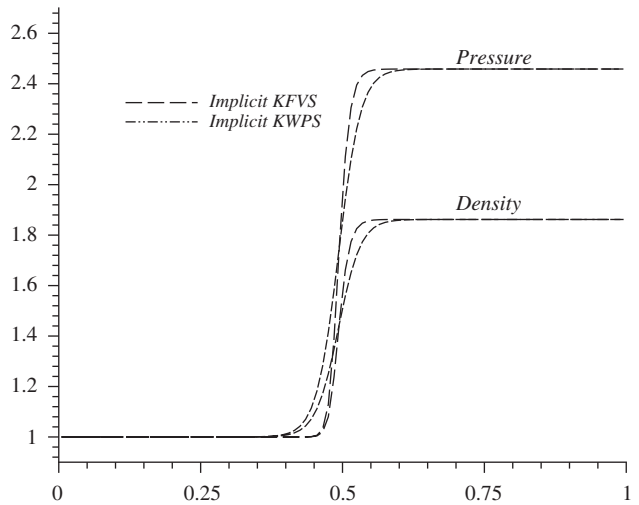

Figure 5. Density & pressure profiles obtained with the implicit schemes for the 1-D shock structure computations.

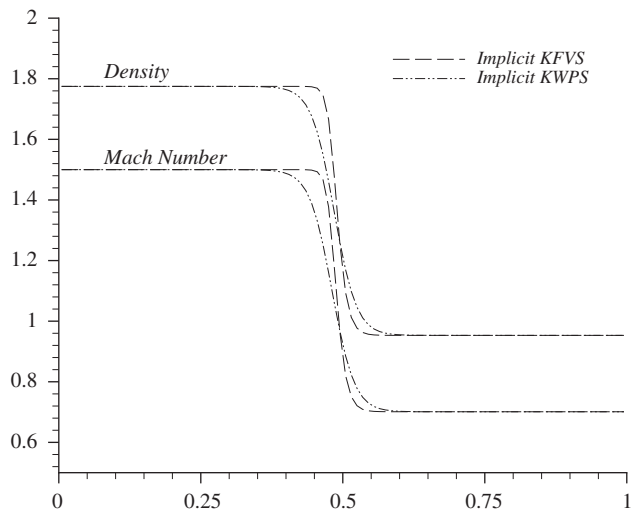

Figure 6. Velocity and Mach number profiles obtained with the implicit schemes for the 1-D shock structure computations.

A closer look at the eigenvalue analysis shows that the Jacobians derived using the continuum approach can have complex eigenvalues, while this is not the case for the Jacobians obtained by the molecular approach [8].

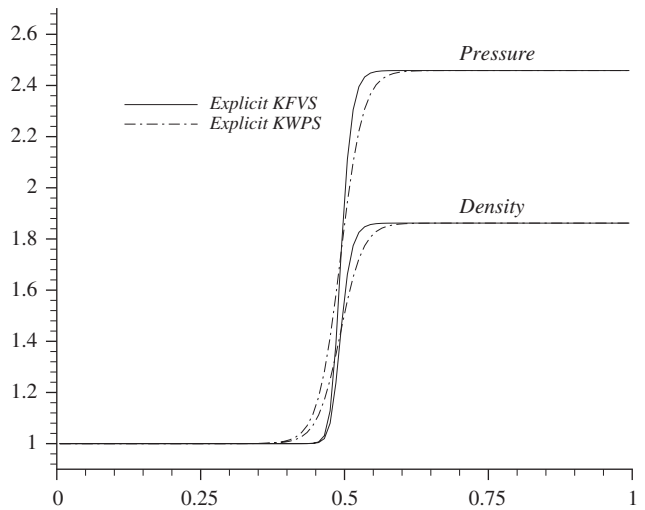

Figure 7. Density and pressure profiles obtained with the explicit schemes for the 1-D shock structure computations.

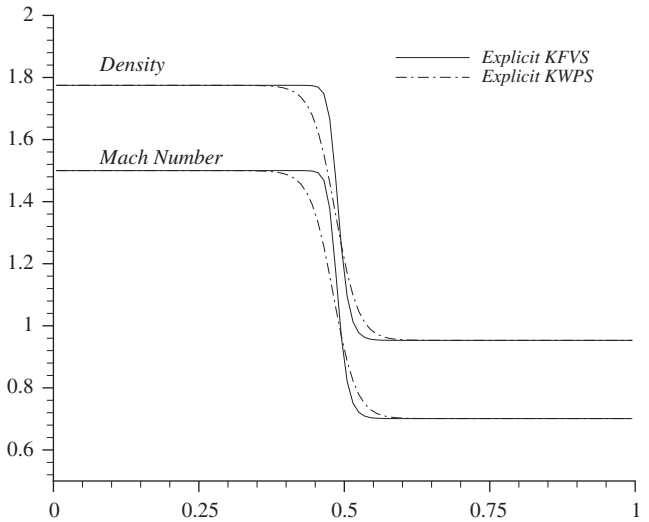

Figure 8. Velocity and Mach number profiles obtained with the explicit schemes for the 1-D shock structure computations.

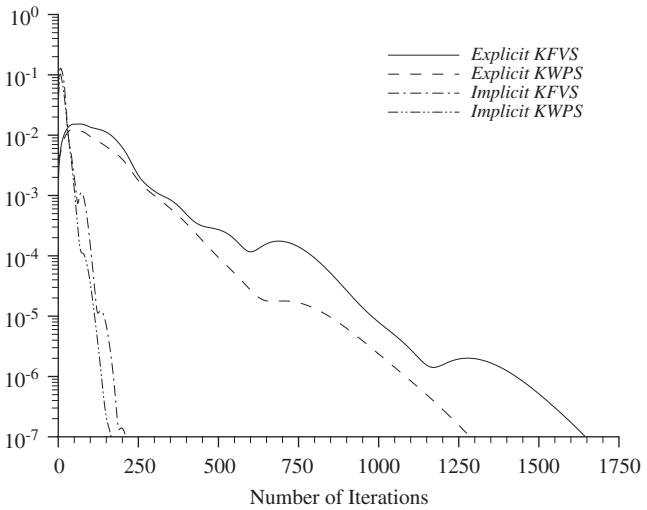

Figure 9. Convergence history for the 1-D shock structure computations.

Table I. Computation time for 1-D shock structure test case.

Numerical scheme	No. of iterations	Comp. time (s)
Explicit KFVS	1646	7.94
Explicit KWPS	1286	2.60
Implicit KFVS	211	4.36
Implicit KWPS	166	2.97

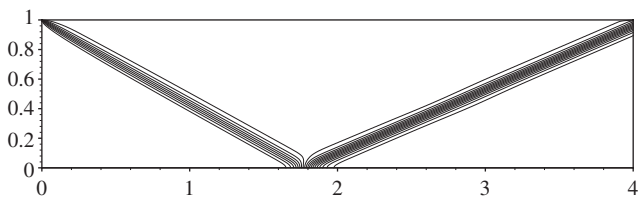

Figure 10. Implicit KFVS calculations of the density contours for 2-D oblique shock reflection from a flat plate.

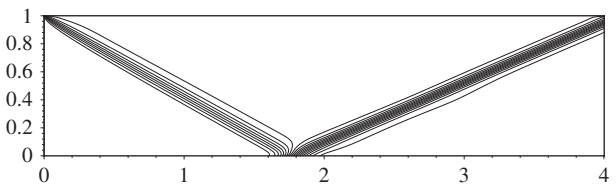

Figure 11. Implicit KWPS calculations of the density contours for 2-D oblique shock reflection from a flat plate.

Table II. Computation time for 2-D oblique shock reflection test case.

Numerical scheme	No. of iterations	Comp. time (s)
Explicit KFVS	2585	2:44:50.53
Explicit KWPS	2828	1:32:37.60
Implicit KFVS	201	1:28:06.43
Implicit KWPS	315	2:07:43.57

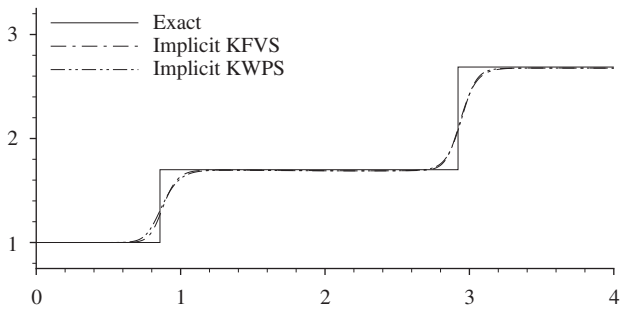

Figure 12. Density profiles along the mid-plane ($y = 0.5$) for 2-D oblique shock reflection from a flat plate using implicit schemes.

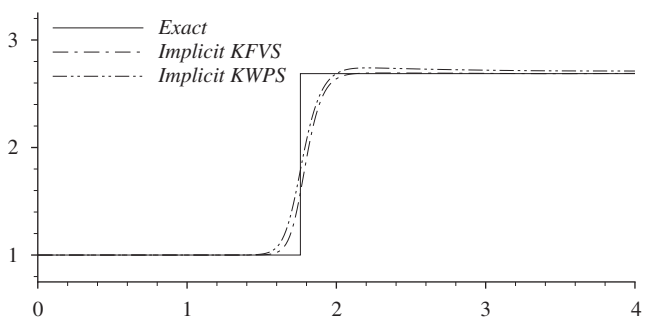

Figure 13. Density profiles along the solid wall for 2-D oblique shock reflection from a flat plate using implicit schemes.

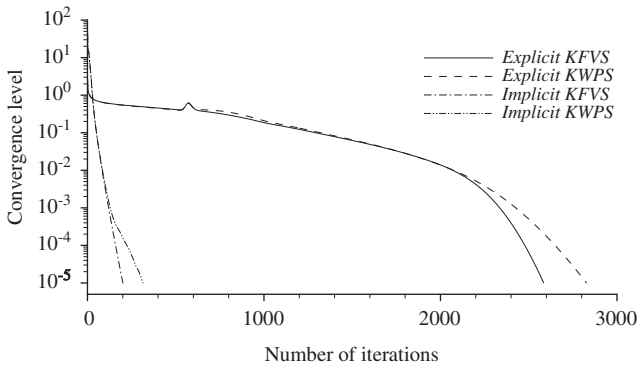

Figure 14. Convergence history for 2-D oblique shock reflection from a flat plate test case.

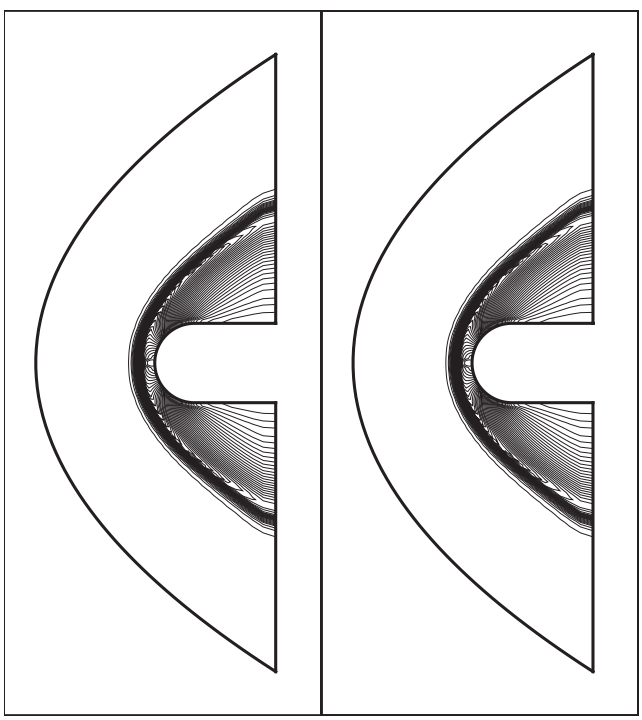

Figure 15. Density contours for the blunt-body computation using explicit (L) and implicit (R) KWPS scheme; $M_\infty = 5.85$, $p_\infty = 510$ Pa, $T_\infty = 55$ K.

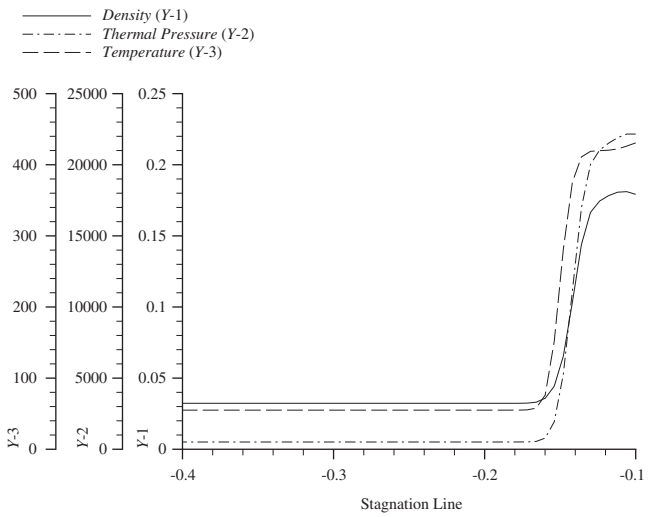

Figure 16. Density, pressure, and temperature profiles along the stagnation line of the blunt-body using explicit KWPS scheme; $M_\infty = 5.85$, $p_\infty = 510\,\text{Pa}$, $T_\infty = 55\,\text{K}$.

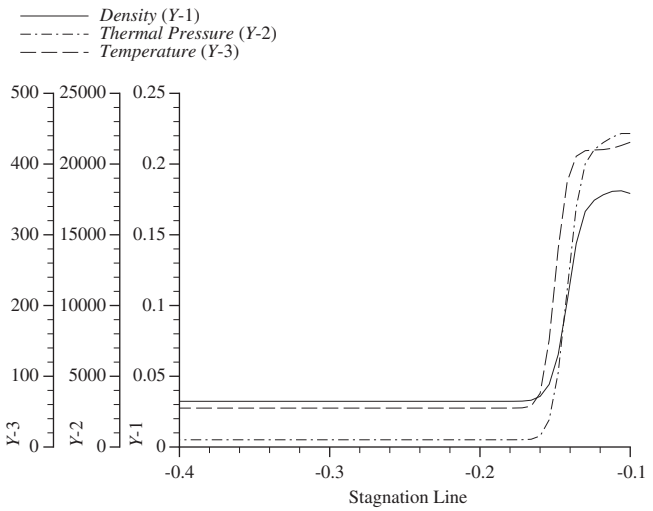

Figure 17. Density, pressure, and temperature profiles along the stagnation line of the blunt-body using implicit KWPS scheme; $M_\infty = 5.85$, $p_\infty = 510\,\text{Pa}$, $T_\infty = 55\,\text{K}$.

5. CONCLUSIONS

Implicit formulations for two kinetic algorithms for Euler flows, namely, the kinetic flux-vector split (KFVS) and the kinetic wave/particle split (KWPS) scheme, have been derived and tested for 1-D and 2-D benchmark test cases. The numerical results indicate an in-

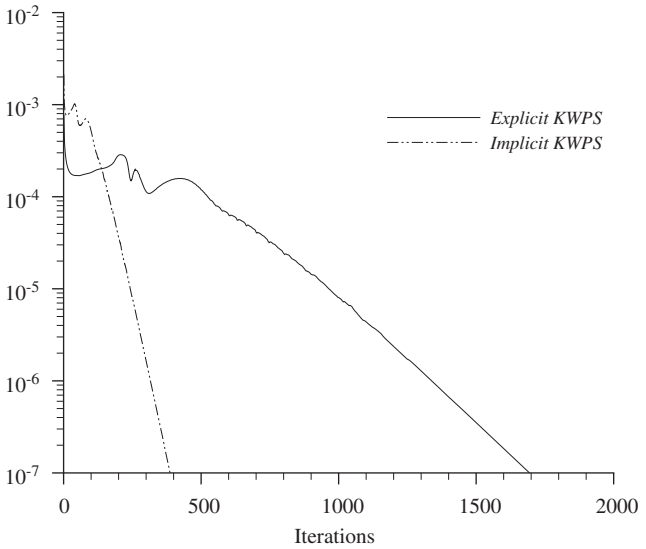

Figure 18. Convergence history for computation of supersonic flow past a blunt-body using the KWPS schemes.

Table III. Computation time for supersonic flow past a 2-D blunt-body test case.

Numerical scheme	No. of iterations	Comp. time (s)
Explicit KWPS	1695	14:54.86
Implicit KWPS	388	1:39:46.31

crease in computational efficiency in obtaining steady state solutions using these new implicit formulations.

NOMENCLATURE

$\mathbf{A}$	Jacobian matrix
c_i	thermal or peculiar velocity
e_t	mass specific total energy ($\equiv q + \frac{1}{\gamma-1}RT$)
$\mathbf{F}$	flux vector
f	probability density distribution function
$f^{(0)}$	Maxwellian probability density distribution function
$\mathbf{I}$	identity matrix
$J(f,f)$	collision integral
KFVS	kinetic flux-vector split
KWPS	kinetic wave/particle split

p pressure
$\mathbf{Q}$ field vector
q mass specific kinetic energy ($\equiv \frac{1}{2}u_k u_k$)
S_i velocity ratio ($\equiv u_i\sqrt{\beta}$)
u_i fluid velocity
v_i molecular velocity
β equivalent temperature ($\equiv 1/2RT$)
γ ratio of specific heats
ε internal energy
ε_o average internal energy ($\equiv (1/(\gamma-1)-\frac{3}{2})\frac{1}{2\beta}$)
$\mathbf{\Psi}$ collision invariant vector ($\equiv [1 \;\; v_j \;\; \varepsilon + \frac{1}{2}v_k v_k]^{\mathrm{T}}$)
ρ density

REFERENCES

1. Mandal JC, Deshpande SM. Kinetic flux vector splitting for Euler equations. *Computers and Fluids* 1994; **23**(2):447–478.
2. Agarwal RK, Acheson KE. A kinetic theory based wave/particle flux splitting scheme for the Euler equations. *AIAA* 95-2178, 1995.
3. Balakrishnan N, Deshpande SM. New upwind method exploiting the wave-particle behaviour of fluid flow. *CFD Journal* 1995; **3**(4):433–446.
4. Hoffman KA, Chiang ST. *Computational Fluid Dynamics for Engineers* (2nd edn), vol. II. Engineering Education System: Wichita, KS, 1993.
5. Anderson JD. *Modern Compressible Flow with Historical Perspective* (2nd edn). McGraw-Hill: New York, 1990.
6. Tannehill JC, Anderson DA, Pletcher RH. *Computational Fluid Mechanics and Heat Transfer* (2nd edn). Taylor and Francis: London, 1997.
7. Press WH, Teukolsky SA, Vetterling WT, Flannery BP. *Numerical Recipes in FORTRAN* (2nd edn). Cambridge University Press: Cambridge, 1992.
8. Reksoprodjo HSR. Development of kinetic schemes for the numerical solutions of the 2-D Euler and the ideal magnetohydrodynamics equations. (*PhD. Dissertation*). Wichita State University, 2002.

